

# VIIth Rencontres du Vietnam, Hanoi, August 6-12 2006

## Nanophysics: from fundamentals to applications

### Minimum conductivity and maximum Fano factor in mesoscopic graphene

B. Trauzettel,<sup>1</sup> J. Tworzydło,<sup>2</sup> M. Titov,<sup>3</sup> A. Rycerz,<sup>4</sup> and C.W.J. Beenakker<sup>5</sup>

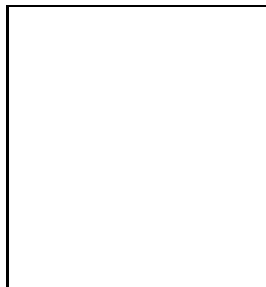
<sup>1</sup>*Department of Physics and Astronomy, University of Basel, 4056 Basel, Switzerland*

<sup>2</sup>*Institute of Theoretical Physics, Warsaw University, 00-681 Warsaw, Poland*

<sup>3</sup>*Department of Physics, University of Konstanz, 78457 Konstanz, Germany*

<sup>4</sup>*Marian Smoluchowski Institute of Physics, Jagiellonian University, 30-059 Kraków, Poland*

<sup>5</sup>*Instituut-Lorentz, Universiteit Leiden, 2300 RA Leiden, The Netherlands*



We calculate the mode-dependent transmission probability of massless Dirac fermions through an ideal strip of graphene (with no impurities or defects), to obtain the conductance and shot noise as a function of Fermi energy. We find that the minimum conductivity of order  $e^2/h$  at the Dirac point (when the electron and hole excitations are degenerate) is associated with a maximum of the Fano factor (the ratio of noise power and mean current). For short and wide graphene strips the Fano factor at the Dirac point equals  $1/3$ , three times smaller than for a Poisson process. The minimum conductivity of order  $e^2/h$  and the Fano factor of  $1/3$  are two remarkable results which indicate that ballistic transport of relativistic electrons at the Dirac point is pseudo-diffusive. This is due to the fact that transport occurs via evanescent modes.

## 1 Introduction

It has recently been observed that the conductivity of graphene (a single layer of carbon atoms) tends to a minimum value of the order of the quantum unit  $e^2/h$  when the concentration of charge carrier tends to zero, i.e. when the system is tuned to the charge neutrality point<sup>1,2</sup>. This minimum conductivity is an intrinsic property of two-dimensional Dirac fermions which persists in an ideal crystal without any impurities or lattice defects<sup>3,4,5,6,7</sup>. Although the origin of the minimum conductivity of graphene is qualitatively well understood, a quantitative explanation of experimental observations is still lacking. It is expected that disorder plays a crucial role<sup>8,9,10,11,12</sup> since most of the experiments (up to now) have been carried out with samples in

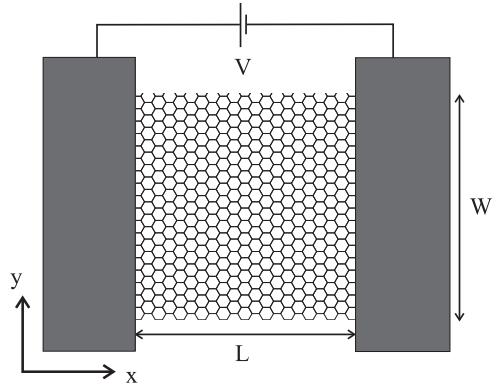


Figure 1: Schematic of a strip of graphene of width  $W$ , contacted by two electrodes (black rectangles) at a distance  $L$ . A voltage source (with bias  $V$ ) drives a dc current through the strip. A separate gate electrode (not shown) allows the carrier concentration in the strip to be tuned around the neutrality point. We analyze transport properties for different types of boundary conditions in  $y$ -direction.

the quasi-ballistic regime. The only reported exception we know about is a measurement of proximity-induced supercurrent in single layer graphene<sup>13</sup>, where the superconducting electrodes are separated by about 200 nm.

In the absence of impurity scattering, and at zero temperature, one might expect the electrical current to be noiseless. In contrast, we have shown in Ref.<sup>7</sup> that the minimum in the conductivity is associated with a maximum in the Fano factor (the ratio of noise power and mean current). The Fano factor at zero carrier concentration takes on the universal value  $1/3$  for a wide and short graphene strip. This is three times smaller than the Poissonian noise in a tunnel junction and identical to the value in a disordered metal<sup>14,15</sup> – even though the classical dynamics in the graphene strip is ballistic. The reason is that electron transport at the Dirac point happens via evanescent modes and not via propagating modes as it is usually the case in ballistic systems.

Shot noise measurements have proven to be a valuable diagnostic tool in carbon nanotubes, which can be thought of as rolled-up sheets of graphene. Very low shot noise in well-contacted bundles of single-wall nanotubes is an indication of nearly ballistic one-dimensional transport<sup>16</sup>. Super-Poissonian noise has been found in a quantum dot formed out of a single-wall nanotube, and explained in terms of inelastic tunneling in this zero-dimensional system<sup>17</sup>. Our prediction of sub-Poissonian shot noise in two-dimensional graphene is another manifestation of the importance of dimensionality for quantum transport. Up to now, shot noise measurements in graphene have not been reported.

The analysis of Ref.<sup>7</sup> was inspired by an insightful paper of Katsnelson<sup>6</sup>, who used the Landauer transmission formula to obtain the quantum-limited conductivity. Following the same approach, we calculated the transmission probabilities of Dirac particles through a strip of graphene in the geometry of Fig. 1. (An earlier study of the same geometry counted the number of propagating modes, without determining their transmission probabilities<sup>18</sup>.) The result depends on the aspect ratio  $L/W$  of the strip and also on microscopic details of the upper and lower edge. We will show below that for short and wide strips ( $L/W \ll 1$ ) these microscopic details become insignificant.

The present paper reviews the theory of Ref.<sup>7</sup>. In Sec. 2, we introduce our model of a ballistic strip of graphene contacted by two electrodes. Then, in Sec. 3, we discuss transport properties such as the conductance and the shot noise of this system. Finally, we conclude in Sec. 4.

## 2 Model

We first discuss the model for graphene nanoribbons with edges which are smooth on the scale of the lattice spacing and later on consider the case of an atomically sharp edge. The band structure of graphene has two valleys, which are decoupled in the case of a smooth edge. In a given valley the excitations have a two-component envelope wave function  $\Psi = (\Psi_1, \Psi_2)$ , varying on scales large compared to the lattice spacing. (The accuracy of this continuum description of the electronic states in graphene is well established<sup>19</sup>.) The two components refer to the two sublattices in the two-dimensional hexagonal lattice of carbon atoms. (The additional spin degeneracy of the excitations does not play a role here.) The wave equation for  $\Psi$  is the Dirac equation,

$$[vp_x\sigma_x + vp_y\sigma_y + v^2M(y)\sigma_z + \mu(x)]\Psi(\mathbf{r}) = \varepsilon\Psi(\mathbf{r}), \quad (1)$$

with  $v$  the velocity of the massless excitations of charge  $e$  and energy  $\varepsilon$ ,  $\mathbf{p} = -i\hbar\partial/\partial\mathbf{r}$  the momentum operator,  $\mathbf{r} = (x, y)$  the position, and  $\sigma_i$  a Pauli matrix.

The mass term  $M(y)$  is zero in the interior of the strip and rises to  $\infty$  at the edges  $y = 0$  and  $y = W$ , thereby confining the particles. As shown by Berry and Mondragon<sup>20</sup>, infinite mass confinement corresponds to the boundary condition

$$\Psi_1|_{y=0} = \Psi_2|_{y=0}, \quad \Psi_1|_{y=W} = -\Psi_2|_{y=W}. \quad (2)$$

As a result of this boundary condition, the transversal momenta are quantized as

$$q_n = \frac{1}{W}\pi\left(n + \frac{1}{2}\right), \quad n = 0, 1, 2, \dots, \quad (3)$$

with  $n$  labeling the modes. The quantization condition for Dirac particles confined by an infinite mass differs from the one for normal electrons confined by an infinite potential by the offset of  $1/2$ , originating from the  $\pi$  phase shift in the boundary condition (2).

The Fermi energy in the sample region  $\mu(x) = \mu$  for  $0 < x < L$  can be varied by a gate voltage  $V_{\text{gate}}$ . It has been experimentally verified that the combined system of graphene and its substrate can be treated to a very good approximation as a parallel plate capacitor<sup>21</sup>. Thus, since then the relation  $en_e = CV_{\text{gate}}$  holds (where  $C$  is the constant capacitance of the plate capacitor) the electron density  $n_e$  is proportional to  $V_{\text{gate}}$ . For a usual two dimensional electron gas (2DEG), the density of states  $D_{\text{2DEG}}(\varepsilon) = \text{const.}$  does not depend on the energy  $\varepsilon$  of the electrons and, therefore,  $n_e \propto \mu$ . For graphene instead (with its relativistic spectrum) the density of states depends linearly on the energy of the electrons  $D_{\text{graphene}}(\varepsilon) \propto \varepsilon$ . Thus,  $n_e \propto \mu^2$  and  $\mu \propto \sqrt{V_{\text{gate}}}$ . The value  $\mu = 0$  corresponds to charge neutrality, being the point where electron and hole excitations are degenerate (known as the Dirac point). We model the electrodes by taking a large value  $\mu(x) = \mu_\infty$  in the leads  $x < 0$  and  $x > L$ . (The parameter  $\mu_\infty$  will drop out of the results, if  $|\mu_\infty| \gg |\mu|$ .) Recently, Schomerus has shown that transport through a sufficiently large sample of graphene close to the Dirac point does not critically depend on most details of the leads<sup>22</sup> (see also Ref.<sup>23</sup> for comparison). This makes us confident that our results are generally valid for ballistic graphene samples with good contacts to metallic leads.

## 3 Conductivity and shot noise

We calculate the transmission probabilities at the Fermi level by matching modes at  $x = 0$  and  $x = L$ . The matching condition for the Dirac equation is the continuity of the two components of  $\Psi$ . This ensures the conservation of the local current density  $\mathbf{j}(\mathbf{r}) = ev\Psi^\dagger(\mathbf{r}) \cdot \boldsymbol{\sigma} \cdot \Psi(\mathbf{r})$ , with  $\boldsymbol{\sigma} = (\sigma_x, \sigma_y)$ . There is a separate transmission probability  $T_n$  for each of the  $N$  propagating modes in the leads, because the matching condition does not mix the modes. (The integer  $N \gg 1$  is given by  $N = \text{Int}\left(k_\infty W/\pi + \frac{1}{2}\right)$ , with  $|\mu_\infty| = \hbar vk_\infty$ .)

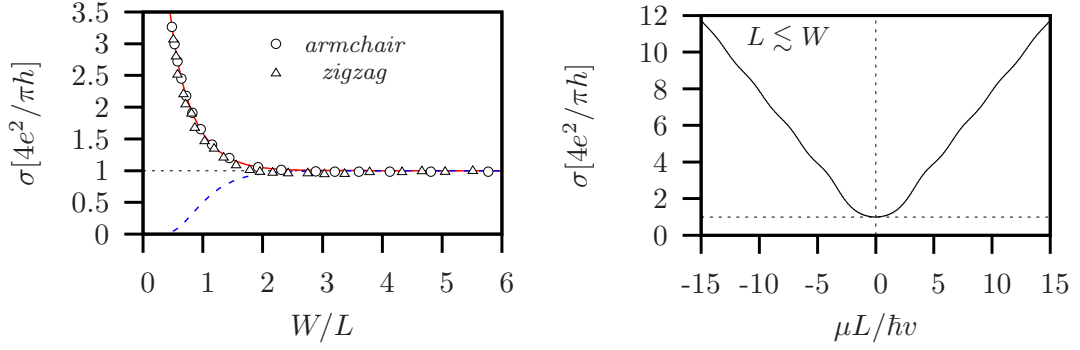


Figure 2: Left panel: The conductivity at the Dirac point ( $\mu = 0$ ), as a function of the aspect ratio of the graphene strip. The curves are calculated from Eq. (6) in the limit  $N \rightarrow \infty$ , for two different boundary conditions: smooth edge [dashed (blue) curve, using Eq. (4)] and “metallic armchair” edge [solid (red) curve, using Eq. (9)]. The limit  $W/L \rightarrow \infty$  (dotted line) is given by Eq. (10), regardless of the boundary condition. The data points for the metallic armchair edge (open circles) and the zigzag edge (open triangles) are the result of a numerical solution of the tight-binding model on a hexagonal lattice. Right panel: Gate voltage dependence of the conductivity for a fixed aspect ratio in the universal regime. The curves are calculated for  $W \gg L$ . At the Dirac point, the conductivity takes its minimum value  $4e^2/\pi h$ . Far away from the Dirac point it increases linearly with  $\mu \propto \sqrt{V_{\text{gate}}}$ .

Details of the calculation are given in the Appendix of Ref. <sup>7</sup>. At the Dirac point  $\mu = 0$  the transmission probability reads

$$T_n = \frac{1}{\cosh^2 Lq_n + (q_n/k_\infty)^2 \sinh^2 Lq_n} \rightarrow \frac{1}{\cosh^2[\pi(n + 1/2)L/W]} \text{ for } N \gg W/L. \quad (4)$$

The formula (4) is essentially different from the textbook formula for the transmission probability of nonrelativistic electrons through a potential barrier, which vanishes in the limit  $N \rightarrow \infty$  at zero energy (relative to the top of the barrier).

The finite transmission probability at the Dirac point tends to the ballistic limit  $T_n \rightarrow 1$  with increasing the carrier concentration in the sample region, i.e. increasing  $|V_{\text{gate}}|$ . For  $N \rightarrow \infty$  we find the expression

$$T_n = \left| \frac{2\kappa^2 - 2(q_n - k_n)^2}{e^{k_n L}(q_n - k_n + i\kappa)^2 + e^{-k_n L}(q_n - k_n - i\kappa)^2} \right|^2, \quad (5)$$

with  $\kappa = |\mu|/\hbar v$  and  $k_n = \sqrt{q_n^2 - \kappa^2}$  for  $q_n > \kappa$  or  $k_n = i\sqrt{\kappa^2 - q_n^2}$  for  $q_n < \kappa$ .

The conductance  $G$  and Fano factor  $F$  follow by summing over the modes,

$$G = g_0 \sum_{n=0}^{N-1} T_n, \quad F = \frac{\sum_{n=0}^{N-1} T_n(1 - T_n)}{\sum_{n=0}^{N-1} T_n}, \quad (6)$$

with  $g_0 = 4e^2/h$ . (The factor 4 accounts for the spin and valley degeneracy.) The dependence of the conductivity

$$\sigma \equiv G \times \frac{L}{W} \quad (7)$$

at  $\mu = 0$  on the aspect ratio  $W/L$  and its dependence on  $\mu$  at a fixed value of  $W/L$  is shown in Fig. 2. Similarly, we show in Fig. 3 the dependence of the Fano factor at  $\mu = 0$  on the aspect ratio  $W/L$  and its dependence on  $\mu$  at a fixed value of  $W/L$ .

Fig. 2 and Fig. 3 also contain results for a boundary condition corresponding to an abrupt edge (dashed curves). We consider a “metallic armchair” edge, in which the carbon lattice

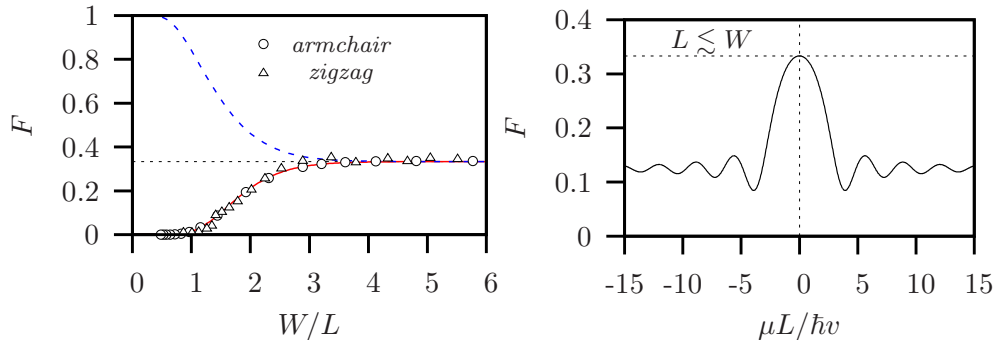


Figure 3: Left panel: The Fano factor at the Dirac point ( $\mu = 0$ ), as a function of the aspect ratio of the graphene strip. The curves are calculated from Eq. (6) in the limit  $N \rightarrow \infty$ , for two different boundary conditions: smooth edge [dashed (blue) curve, using Eq. (4)] and “metallic armchair” edge [solid (red) curve, using Eq. (9)]. The limit  $W/L \rightarrow \infty$  (dotted line) is given by Eq. (10), regardless of the boundary condition. The data points for the metallic armchair edge (open circles) and the zigzag edge (open triangles) are the result of a numerical solution of the tight-binding model on a hexagonal lattice. Right panel: Gate voltage dependence of the Fano factor for a fixed aspect ratio in the universal regime. The curves are calculated for  $W \gg L$ . At the Dirac point, the Fano factor takes its maximum value  $1/3$ . The oscillations (away from the Dirac point) indicate the appearance of propagating modes in the graphene strip with increasing gate voltage.

contains a multiple of three hexagons in the transverse direction, terminated at  $y = 0$  and  $y = W$  by a horizontal bond. This edge mixes the valleys, so we need to consider a four-component wave function  $\Psi = (\Psi_1, \Psi_2, \Psi'_1, \Psi'_2)$ . The first two components satisfy the Dirac equation (1), without the mass term, and the second two components satisfy the same equation with  $p_y \rightarrow -p_y$ . The boundary condition is<sup>19</sup>

$$\Psi_1 = \Psi'_1, \quad \Psi_2 = \Psi'_2, \quad \text{at } y = 0, W. \quad (8)$$

The valley degeneracy is broken for the lowest mode ( $n = 0$ ), which is nondegenerate, while all higher modes ( $n = 1, 2, \dots$ ) retain the twofold valley degeneracy (over and above the twofold spin degeneracy, common to all modes). For  $\mu = 0$  and  $N \rightarrow \infty$  the transmission probabilities are given by

$$T_n = \frac{1}{\cosh^2(\pi n L/W)}, \quad n = 0, 1, 2, \dots \quad (9)$$

The essential difference with the result (4) for the smooth edge is due to the absence of the  $1/2$  offset in the quantization condition of the transverse momentum. The different boundary condition changes the strip from insulating to metallic in the limit  $W/L \rightarrow 0$ , but has no effect in the opposite limit  $W/L \rightarrow \infty$ , cf. Fig. 2.

To test the analytical results from the continuum description of graphene, we have also carried out numerical simulations using the tight-binding model with nearest-neighbor hopping on a honeycomb lattice with metallic armchair edges. We took some 2000 lattice sites for the graphene strip, coupling it to semi-infinite leads at the two ends. The valley degeneracy of modes  $n = 1, 2, \dots$  is now only approximate, but the relative magnitude of the mode splitting vanishes  $\propto a/W$  as the width becomes large compared to the lattice spacing  $a$ <sup>24</sup>. The numerical results, included in Fig. 2 and Fig. 3 are in excellent agreement with the analytical prediction and confirm the universality of the regime  $W/L \gg 1$ .

A comparison of Figs. 2 and 3 shows that the minimum in the conductivity at the Dirac point is associated with a maximum in the Fano factor. The limiting behavior at the Dirac point for a short and wide strip is

$$\sigma \rightarrow g_0/\pi, \quad F \rightarrow 1/3, \quad \text{for } W/L \rightarrow \infty. \quad (10)$$

Note that these limits are already reached for moderate aspect ratios  $W/L \geq 2 - 3$ . We have derived this limiting behavior for two types of boundary conditions (smooth edge and metallic armchair edge), but we are confident that the result is universal, in the sense that it holds for the most general boundary condition at the edges of the graphene strip (as classified in Refs. 25,26).

The result (10) for the minimal conductivity agrees with other calculations<sup>3,4,5</sup>, which start from an unbounded disordered system and then take the limit of infinite mean free path  $l$ . There is no geometry dependence if the limits are taken in that order. In the ballistic bounded system considered here, a geometry dependence persists in the thermodynamic limit<sup>6</sup>. Existing experiments<sup>1,2</sup> are quasi-ballistic, with  $l \simeq W < L$ , finding  $\sigma \approx g_0$ . Thus, our prediction for the minimum conductivity is a factor  $1/\pi$  too small as compared to the measured values in quasi-ballistic systems. Furthermore, we predict that away from the Dirac point the conductivity increases as  $\sqrt{V_{\text{gate}}}$  with increasing gate voltage whereas experiments in the quasi-ballistic regime show a linear increase of  $\sigma$  as a function of  $V_{\text{gate}}$ . The gate voltage dependence away from the Dirac point seen in the experiments<sup>1,2</sup> can be explained by the effect of charged (long-ranged) impurities in the substrate<sup>8</sup> or by strong disorder (in the unitary limit)<sup>9</sup>.

The limit  $F = 1/3$  for the Fano factor is smaller than the value  $F = 1$  expected for a Poisson process. The same  $1/3$  value appears in a disordered metal<sup>14,15</sup>, where it is a consequence of classical diffusive dynamics. This correspondence is remarkable, since in our ideal graphene strip the classical dynamics is ballistic. Therefore, ballistic transport in a short and wide strip of graphene resembles pseudo-diffusive transport at the Dirac point. This result also extends to the case of bilayer graphene, where it has been shown that the Fano factor (at the Dirac point) has the same  $1/3$  value as in a monolayer<sup>27</sup>. The pseudo-diffusive transport property of graphene at the charge neutrality point is a robust phenomenon which even remains in the presence of a magnetic field<sup>28</sup>.

## 4 Conclusions

In conclusion, we predict that the conductance of ballistic graphene at the Dirac point has a  $1/L$  dependence, where  $L$  is the distance of the electrodes in contact with a strip of graphene. This is an unexpected result since usually the conductance of a ballistic sample is independent of  $L$ . The reason is that transport at the Dirac point happens through evanescent and not through propagating modes. Furthermore, we show that electrical conduction through an ideal strip of graphene is associated with time-dependent current fluctuations — at zero temperature and without any impurities or lattice defects. The electrical noise is largest, relative to the mean current, when the Fermi energy is adjusted such that electrons and holes are degenerate. At the Dirac point the Fano factor (ratio of noise power and mean current) takes on the universal value  $1/3$  for short and wide strips. Observation of this quantum-limited shot noise would be a unique demonstration of electrical noise produced by relativistic quantum dynamics.

## Acknowledgments

We thank Ya. M. Blanter, H. A. Fertig, H. B. Heersche, P. Jarillo-Herrero, A. F. Morpurgo, and L. M. K. Vandersypen for interesting discussions. The research was supported by the Swiss NSF, the NCCR Nanoscience, the Dutch Science Foundation NWO/FOM, the Polish Science Foundation, and the European Community's Marie Curie Research Training Network (contract MRTN-CT-2003-504574, Fundamentals of Nanoelectronics).

## References

1. K. S. Novoselov, A. K. Geim, S. V. Morozov, D. Jiang, M. I. Katsnelson, I. V. Grigorieva, S. V. Dubonos, and A. A. Firsov, *Nature* **438**, 197 (2005).
2. Y. Zhang, Y.-W. Tan, H. L. Stormer, and P. Kim, *Nature* **438**, 201 (2005).
3. A. W. W. Ludwig, M. P. A. Fisher, R. Shankar, and G. Grinstein, *Phys. Rev. B* **50**, 7526 (1994).
4. K. Ziegler, *Phys. Rev. Lett.* **80**, 3113 (1998).
5. N. M. R. Peres, F. Guinea, and A. H. Castro Neto, *Phys. Rev. B* **73**, 125411 (2006).
6. M. I. Katsnelson, *Eur. Phys. J. B* **51**, 157 (2006).
7. J. Tworzydło, B. Trauzettel, M. Titov, A. Rycerz, and C.W.J. Beenakker, *Phys. Rev. Lett.* **96**, 246802 (2006). An extended version of the paper with details of the calculation can be found in cond-mat/0603315 (2006).
8. K. Nomura and A. H. MacDonald, cond-mat/0606589 (2006).
9. P. M. Ostrovsky, I. V. Gornyi, and A. D. Mirlin, *Phys. Rev. B* **74**, 235443 (2006).
10. H. Kumazaki and D. S. Hirashima, *J. Phys. Soc. Jpn.* **75**, 53707 (2006).
11. T. Ando, *J. Phys. Soc. Jpn.* **75**, 74716 (2006).
12. M. Titov, cond-mat/0611029 (2006).
13. H. B. Heersche, P. Jarillo-Herrero, J. B. Oostinga, L. M. K. Vandersypen, and A. F. Morpurgo, cond-mat/0612121 (2006).
14. C. W. J. Beenakker and M. Büttiker, *Phys. Rev. B* **46**, 1889 (1992).
15. K. E. Nagaev, *Phys. Lett. A* **169**, 103 (1992).
16. P.-E. Roche, M. Kociak, S. Guéron, A. Kasumov, B. Reulet, and H. Bouchiat, *Eur. Phys. J. B* **28**, 217 (2002).
17. E. Onac, F. Balestro, B. Trauzettel, C. F. J. Lodewijk, and L. P. Kouwenhoven, *Phys. Rev. Lett.* **96**, 026803 (2006).
18. N. M. R. Peres, A. H. Castro Neto, and F. Guinea, *Phys. Rev. B* **73**, 195411 (2006).
19. L. Brey and H. A. Fertig, *Phys. Rev. B* **73**, 235411 (2006).
20. M. V. Berry and R. J. Mondragon, *Proc. R. Soc. Lond. A* **412**, 53 (1987).
21. K. S. Novoselov, A. K. Geim, S. V. Morozov, D. Jiang, Y. Zhang, S. V. Dubonos, I. V. Grigorieva, and A. A. Firsov, *Science* **306**, 666 (2004).
22. H. Schomerus, cond-mat/0611209 (2006).
23. Ya. M. Blanter and I. Martin, cond-mat/0612577 (2006).
24. The magnitude of the mode splitting follows from the formulas given in the appendix of K. Wakabayashi, M. Fujita, H. Ajiki, and M. Sigrist, *Phys. Rev. B* **59**, 8271 (1999).
25. E. McCann and V. I. Fal'ko, *J. Phys. Condens. Matter* **16**, 2371 (2004).
26. A. R. Akhmerov and C. W. J. Beenakker, cond-mat/0612698 (2006).
27. I. Snyman and C. W. J. Beenakker, cond-mat/0609243 (2006); to be published in *Phys. Rev. B* (2007).
28. E. Prada, P. San-Jose, B. Wunsch, and F. Guinea, cond-mat/0611189 (2006).